Characteristics of Airborne Ultrafine and Coarse Particles during the Australian Dust Storm of 23 September 2009

E.R. Jayaratne, G.R. Johnson, P. McGarry, H.C. Cheung and L. Morawska*

International Laboratory for Air Quality and Health

Queensland University of Technology

GPO Box 2434, Brisbane, QLD 4001, Australia

Revised and Submitted to

Atmospheric Environment

Apr 2011

* Corresponding author contact details:

Tel: (617) 3138 2616; Fax: (617) 3138 9079

Email: l.morawska@qut.edu.au

Abstract

Particle number concentrations and size distributions, visibility and particulate mass concentrations and weather parameters were monitored in Brisbane, Australia, on 23 September 2009, during the passage of a dust storm that originated 1400 km away in the dry continental interior. The dust concentration peaked at about mid-day when the hourly average $PM_{2.5}$ and PM_{10} values reached 814 and 6460 μg m^{-3}, respectively, with a sharp drop in atmospheric visibility. A linear regression analysis showed a good correlation between the coefficient of light scattering by particles (Bsp) and both PM_{10} and $PM_{2.5}$. The particle number in the size range 0.5-20 μm exhibited a lognormal size distribution with modal and geometrical mean diameters of 1.6 and 1.9 μm, respectively. The modal mass was around 10 μm with less than 10% of the mass carried by particles smaller than 2.5 μm. The PM_{10} fraction accounted for about 68% of the total mass. By mid-day, as the dust began to increase sharply, the ultrafine particle number concentration fell from about $6x10^3$ cm^{-3} to $3x10^3$ cm^{-3} and then continued to decrease to less than $1x10^3$ cm^{-3} by 14h, showing a power-law decrease with Bsp with an R^2 value of 0.77 ($p<0.01$). Ultrafine particle size distributions also showed a significant decrease in number during the dust storm. This is the first scientific study of particle size distributions in an Australian dust storm.

Keywords: *Dust storm, Particle Concentration, Particle Size, Visibility, Air Pollution*

1. Introduction

Dust storms occur when high winds caused by pressure gradients whip up loose soil over a large area and transport it across the land. When the wind speed reaches a threshold value, sand and dust particles on the surface of the ground begin to vibrate and are ejected into the air – a process known as 'saltation'. The impact of these windborne particles on the surface ejects yet more particles and causes a chain reaction. Ejected sands and dust can be transported by wind to great distances and, In addition to reduced visibility that affects air and road transport, dust storms cause soil erosion and loss of organic matter and nutrients from the soil (Wang et al., 2006).

From the point of view of human health, people with breathing-related problems, such as asthma and emphysema, have been known to experience difficulties during severe dust storms. Lei et al (2004) demonstrated that particulate matter in an Asian dust storm increased lung inflammation and injury in pulmonary hypertensive rats. However, other studies have shown that human mortality rates were not elevated during dust storm days and attributed this to the absence of toxicity in crustal particles (Hefflin et al., 1994; Schwartz et al., 1999).

Fine particles in the air are scavenged by larger particles. This process of coagulation can lead to a shift of average particle size to larger values, especially when the number concentration of particles is high (Matsoukas and Friedlander, 1991). Urban environments are dominated by particles from motor vehicle exhaust, with the large majority of them being in the ultrafine size range, that is - smaller than 0.1 μm (Shi et al., 1999). A detailed account of the characteristics of ultrafine particles in urban environments may be found in the two recent reviews by Morawska et al. (2008) and Kumar et al. (2010). Thus, the passage of a dust storm across a major city offers an ideal opportunity

to investigate the coagulation process between two distinctly different particle size groups in the outdoor environment.

Air quality monitoring stations routinely measure particulate mass in accordance with the respective national ambient air quality standard requirements and normally record this quantity as PM_{10} or $PM_{2.5}$ - the mass concentration of particles smaller than 10 μm or 2.5 μm, respectively. This has enabled a considerable amount of research addressing particle mass concentrations during the passage of dust storms. For example, Zhang et al (2006) monitored particles in the 20 March 2002 dust storm in Beijing, China, and showed that the peak total suspended particle concentration reached 12,000 μg m^{-3} while the mass concentrations of coarse particles accounted for 91% of the total, compared to 61% on non-dust storm days. Choi and Choi (2008) measured particulate mass concentrations at the ground during a dust storm in Kangnung, Korea on 8 March 2004 and showed that PM_{10} concentrations reached 340 μg m^{-3}. They also found that most of the particles were in the range between $PM_{2.5}$ and PM_{10}. Several other studies have confirmed that the average particle size in a dust storm occur in the size range 2-6 μm (Abdulla et al, 1988; Mikami et al, 2005; Kobayashi et al, 2007). Wang et al (2008) used aircraft measurements during the 2006 dust storms over the coastal areas in Northern China and reported that number concentrations of ultrafine particles exceeded 10^5 cm^{-3}. While, data on particle number distributions in dust storms is sparse, measurements of ultrafine particles during dust storm episodes is highly limited.

The continental interior of Australia is a major global source region for atmospheric dust. However, unlike dust and sand storms that occurs regularly in many parts of the world such as in Northern China and the Sahara, Australian dust storms require a specific sequence of environmental conditions. During heavy rain episodes, flood waters from Queensland flow south and deposit large

quantities of fluvial sediments over a large area of the continental interior in and around the Lake Eyre Basin (see map in Fig 1). Such intense flood events followed by prolonged drought conditions can then lead to a significant erosion of alluvial dust with the onset of strong winds that generally occur around September-November (Mitchell et al., 2010). In contrast to the composition of dust in other parts of the world, Australian desert dust is particularly rich in iron which gives it its typical reddish hue, while halites from dry salt lakes comprise about 0.5% by mass (Radhi et al, 2010).

2. Methods

2.1 Overview and Aims

On the 22nd and 23rd September 2009, a large amount of dust was swept up in strong winds caused by an intense low-pressure zone near Lake Eyre and was very quickly carried eastwards and northwards (Fig 1). The ensuing dust storm was estimated to be the worst in 70 years (AGBM, 2010). At its peak, the dust plume was more than 3400 km long and stretched from southern New South Wales to far north Queensland. Airborne particle concentrations of over 15,000 µg m-3 were recorded at many locations. It is estimated that 1.6 x 109 kg of dust was removed from the continental interior which at one time was losing 7.5 x 107 kg h-1 of dust off its eastern coastline (Leys et al., 2009). The region affected by the dust included the state capitals of Sydney and Brisbane. The dust reached Brisbane at a distance of about 1400 km from its source at around 11 am on the 23rd and by 12 noon, resulted in a drop in visibility to a few metres. Dust in the air gave the environment an eerie red-orange colour and the air temperature dropped by several degrees.

The International Laboratory for Air Quality and Health (ILAQH) at the Queensland University of Technology was carrying out measurements of airborne particles at the top of two buildings in the Central Business District of Brisbane when the dust storm passed over the city. The aim of this paper

is to use the results obtained to investigate the physical characteristics of the dust particles as well as to assess the impact of the dust on the regular ultrafine particle number and mass concentrations in an urban environment.

2.2 Monitoring Sites

As this was not a planned experiment, not all instruments were operative right through the dust storm and not all at the same location. The measurements were carried out at two locations, to be denoted Site A and Site B, being two buildings in the Brisbane Central Business District (CBD), separated by a distance of about 0.5 km. Site A was located in a six-floor building within the Gardens Point campus of the Queensland University of Technology, approximately 100m away and midway between a busy freeway and the City Botanical Gardens. The air was sampled from outside a 6th floor window. This site also included an air monitoring station operated by the Queensland Department of the Environment and Resource Management (DERM). Site B was located in a five-floor building situated next to a city street with the air sampled from outside the 5th floor. Therefore, both monitoring sites could be regarded as urban environments, normally dominated by vehicular emissions.

2.3 Instrumentation

The following particle measuring instruments were used in this study:

The TSI 3320 Aerodynamic Particle Sizer (APS) is an optical time-of-flight spectrometer that provides real time high-resolution particle sizing from 0.5 to 20 μm. A complete size distribution, in 52 size bins within the detection range, was obtained every 1 min.

The TSI 3782 water-based Condensation Particle Counter (CPC) measures ultrafine particle number concentration down to a size of 10 nm at concentrations up to $5x10^4$ cm^{-3}. Readings were taken every 1 s and the software was programmed to log average values at intervals of 5 s.

The TSI 8520 DustTrak Aerosol Monitor is a portable laser photometer that measures and records airborne dust concentration from 1 to 10^5 μg m^{-3}. The DustTrak is calibrated against a gravimetric reference using the respirable fraction of standard ISO Arizona test dust which has a wide size distribution covering the entire size range of the DustTrak and is representative of a wide variety of ambient aerosols (TSI, 1997). An inlet impactor was used to restrict the sampled particle mass to an upper size of 2.5 μm ($PM_{2.5}$). Readings were taken every 1 s and the instrument was set to log average values at intervals of 30 s.

Using $PM_{2.5}$ data obtained during the dust storm, the DustTrak was calibrated against a tapered element oscillating microbalance (TEOM) located at Site A. The TEOM is an instrument that is certified by the US-EPA for gravimetric measurements of particulate matter in ambient air. These results are shown in the Supplementary Material of this paper.

A TSI 3936 Scanning Mobility Particle Sizer (SMPS) comprising a 3080 electrostatic classifier and a 3010 CPC was used to obtain particle size distributions in the size range 4 to 100 nm in 91 size bins. A complete scan was derived every 10 min in real time.

Table 1 shows the location and times of operation of the various instruments. While the APS and SMPS were located at Site A, the CPC and DustTrak were located at Site B. These locations were not selected but, with the exception of the APS, the instruments happened to be operating there on other projects as the dust storm approached. It is unfortunate that the APS was not switched on until 16h. Meteorological, visibility and PM_{10} concentrations were monitored at the roof level of the building at the DERM air monitoring station at Site A. The meteorological parameters included air temperature, relative humidity, wind speed and direction. Visibility was monitored with an

integrating nephelometer that measured the atmospheric light scattering coefficient of particles (Bsp) and expressed it in Mm^{-1}. Particulate matter concentration in the form of PM_{10} was recorded with a TEOM at Site A. Hourly average data of the meteorological conditions, visibility and PM_{10} values were also obtained from several ground-level DERM monitoring stations around the city of Brisbane.

2.4 Data Analysis

The data on the CPC, APS, DustTrak were logged in real time at 1 s intervals. The DERM data were available as 30 min averages. Linear regression analysis was used to determine the correlation coefficients between half-hourly PM_{10} and $PM_{2.5}$ values and the corresponding Bsp values. The SMPS and APS data were processed and analysed using Aerosol Instrumentation Manager Software from TSI.

3. Results and Discussion

3.1 Overview of the dust episode

The morning of the 23rd September 2009 was a typical fine spring day in Brisbane. At 8 am, the air temperature was 23ºC and the relative humidity just over 60%. A steady gentle breeze of 0.4 m s^{-1} blew in from the west. Ambient particle concentration was normal with a PM_{10} level of 21 µg m^{-3} and a Bsp of 22 Mm^{-1} at Site A. However, by about 10 am, with dust being transported in by the westerly winds, the PM_{10} had exceeded 100 µg m^{-3}, while the visibility had deteriorated, almost doubling the Bsp to 41 Mm^{-1}. The Australian ambient air quality standard for PM_{10} averaged over 24 hours is 50 µg m^{-3}. By 11 am, the effects of the dust storm were clearly visible. Conditions continued to

deteriorate rapidly in the next hour. Maximum dust levels were observed near mid-day with the Bsp exceeding 1000 Mm^{-1}. Thereafter, the visibility continued to improve steadily with the Bsp dropping sharply until 17h and at a slower rate thereafter. By midnight, there was still a considerable amount of dust in the air, as evidenced by the Bsp value of 83 Mm^{-1}. The real time variation of Bsp in Figure 2 shows the passage of the dust storm over Brisbane. It is instructive to note that the Bsp in Brisbane on a normal day is 10-30 Mm^{-1}.

3.2 DustTrak Accuracy

Figure 3 shows the half-hourly averaged $PM_{2.5}$ data from the DustTrak at Site B and the TEOM at Site A, obtained between 12:30 h and 15:30 h which corresponds to the time period when the dust was most concentrated on the day of the dust storm. The two parameters are plotted against each other. Despite the separation of about 0.5 km between the two sites, the slope of the best line is very close to 1 (0.99 with R^2 = 0.99) showing excellent agreement between the two parameters. This result indicates that the material of the dust was very similar to the Arizona Dust that is used to calibrate the DustTrak (TSI, 1997) and provides confidence that the DustTrak data may be used as a reasonably accurate measure of the $PM_{2.5}$ particulate matter concentration in the dust storm.

3.3 Particulate Mass Concentrations

Figure 4 shows the hourly average particulate mass concentrations between 10h and 16h. The time axis shows the end-hour of each data bin. Thus, for example, the maximum average $PM_{2.5}$ and PM_{10} values of 814 and 6460 µg m^{-3}, respectively, were observed during the hour between 12-13h. It is clear that most of the particulate mass in the size range below 10 µm lay between 2.5 µm and 10 µm.

3.4 Larger Particles

Figure 5(a) shows the particle number size distribution as measured with the APS at 16h. Note that particles smaller than 0.5 μm are not included in this figure. The total APS particle number concentration was 17.3 cm^{-3} and exhibited a near-lognormal size distribution with modal and geometrical mean diameters of 1.6 and 1.9 μm, respectively. The particle volume size distribution (Figure 5(b)) shows that most of the particle volume and, hence, mass was contributed by particles larger than 2.5 μm. The modal mass was around 10 μm. A cumulative analysis showed that less than 10% of the mass was carried by particles smaller than 2.5 μm, while the PM_{10} fraction accounted for about 68% of the total mass. However, these comparisons should be treated with caution, as the APS software calculates the volume from the size assuming that the particles are spherical.

3.5 Ultrafine Particle Number Concentration

Next, we look at the impact of the dust on the ultrafine particle number concentrations. It has been shown that the large majority of ultrafine particles in urban settings are combustion aerosols from vehicle emissions (Shi et al., 1999; Wahlin et al., 2001). Most of these particles are smaller than 200 nm, which is less than one-tenth the size of particles in the dust storm. This gives rise to a process of polydisperse coagulation whereby smaller particles diffuse to the surface of larger particles. A tenfold difference in particle size produces a threefold increase in coagulation (Hinds, 1982). Coagulation generally leads to a reduction in small particle number with no change to the particle mass concentration.

On dust-free days, prior to the event day, the ultrafine particle number concentrations at both measurement sites were typically of the order of $1x10^4$ cm^{-3}. Average values peaked between $1x10^4$ and $3x10^4$ cm^{-3} during the peak traffic hours and dropped to about $5x10^3$ cm^{-3} in the early hours of

the morning. The mean daytime concentration on the day immediately prior to the dust storm, 22nd September, was $1.2x10^4$ cm^{-3}. On the 23rd, after a normal peak number concentration of about $1.5x10^4$ cm^{-3} during the morning traffic peak, the concentration as measured by the CPC at Site B stabilised at around $6x10^3$ cm^{-3} by mid-morning. Figure 6 shows the ultrafine particle number concentration together with the $PM_{2.5}$ measured at the same location between 10h and 15h. The $PM_{2.5}$ curve clearly shows the arrival and passage of the dust. At 11h, as the $PM_{2.5}$ value began to increase sharply, the particle number concentration showed the expected decrease. Particle number concentration values fell from about $5x10^3$ cm^{-3} at 11h to less than $3x10^3$ cm^{-3} by 12h at the peak of the storm. This initial sharp decrease in ultrafine concentration coincided with the arrival of the main dust storm peak. However the ultrafine particle number concentration then continued to decrease at a slower rate even after the dust concentration had begun to decline. These observations suggest that coagulation scavenging of the ultrafine particles was accompanied by a second unidentified process, and that both acted simultaneously to reduce the ultrafine particle number concentration. Right through the time period depicted in Figure 6, the wind remained WSW ($250^oTN \pm 15^o$) at a fairly steady 4.5 ± 0.5 m s^{-1}. Air temperature was $26^o \pm 1^o$ while the relative humidity dropped steadily from about 50% at 10h to about 16% at 15h. Thus, it is unlikely that any change in particle number concentration or particle size was due to a changing air mass other than for the dust from the south-west. In support of the modelling studies that have shown that fine mode particles are scavenged by larger particles in the environment (Ackermann et al., 1998; Jung et al., 2002), the present study demonstrates that the effect can be very effective in a real life dust storm situation.

Next, we investigate the effect of PM_{10} on the ultrafine particle number concentration. Figure 7 shows the hourly average ultrafine particle number concentration against the corresponding PM_{10} concentration between 7h and 16h on the 23rd September. The graph shows a sharp decrease in

ultrafine particle number concentration as the PM_{10} concentration increased. The ultrafine particle number concentration showed a power-law decrease with PM_{10} with an R^2 value of 0.73 ($p<0.01$).

Bsp and PM Correlations

In Figure 8, we look at correlations between the light scattering coefficient of particles (Bsp) and the particulate matter concentrations, PM_{10} and $PM_{2.5}$. Figure 8(a) shows the hourly particulate matter concentrations against Bsp, between 7h and 16h on the 23rd September. A linear regression analysis showed a good correlation between Bsp and both PM_{10} and $PM_{2.5}$, with an R^2 value of 0.98 ($p<0.01$) for each. Fine particles in the size range 0.4 to 0.7 μm that corresponds to the visible spectral wavelength are more efficient at scattering light than other sizes. As this range falls within the size ranges of both PM_{10} and $PM_{2.5}$, it is not surprising that they both correlate well with Bsp.

Figure 8(b) shows the corresponding hourly average ultrafine particle number concentration measured by the CPC as a function of Bsp. In accordance with Figure 4, this graph showed a sharp decrease in particle number concentration as the dust arrived and the Bsp increased. The particle number concentration showed a power-law decrease with Bsp with an R^2 value of 0.77 ($p<0.01$).

As stated, the APS was switched on soon after 16h and continued to sample until 10h on the next day. Figure 9 shows the particle number concentration and geometrical mean diameter as measured between 16h and 24h. If we disregard the peak at around 18h, which was no doubt associated with increased road dust from vehicular traffic in the evening rush hour, we see that the number concentration dropped steadily from about 16 cm^{-3} to about 5 cm^{-3} during this period. Over the same period, the hourly average Bsp and PM_{10} dropped from about 280 Mm^{-1} to 85 Mm^{-1} and from

1300 μg m^{-3} to 400 μg m^{-3}, respectively (Figures 2 and 4). It is interesting to note that, from 16h to 24h, all three parameters decreased by the same factor of just over 3. This was only possible if the particle size did not show a significant difference in time and this is substantiated by the time series graph of the particle diameter in Figure 9. There are twelve outlier points seen in the graph close to 20.30h and 23.00h, which are clearly due to spurious effects as they fall well above the expected variation of the long term readings. Excluding these twelve points, the APS particle geometrical mean diameter over this period was 1.9 ± 0.1 μm, where the uncertainty is the standard deviation. Thus, we see that the variation of the particle diameter about its mean value was no more than about 5%. The slight increase at night-time was probably caused by hygroscopic growth and/or particle coagulation, both phenomena that have been observed in the environment. Right through the time period depicted in Figure 9, the wind remained WSW (255^{o}TN ± 10^{o}) at a fairly steady 4.5 ± 1.0 m s^{-1}.

3.6 Ultrafine Particle Size Distribution

Figure 10 shows the ultrafine particle size distributions before and during the dust storm as measured by the SMPS. Each curve is the average of 12 scans over a full two-hour period. The upper curve reflects the size distribution prior to the arrival of the dust between 8 and 10 am. During this time, the particle mass concentration values were as on any other day, indicating no excess dust in the atmosphere. As the dust arrived, the ultrafine particle numbers decreased. This reduction was very pronounced for ultrafine particles in the size range close to 100 nm but decreased at smaller sizes, with no significant drop in number being detected for particles smaller than 20 nm. This latter range is generally occupied by nanoparticles produced by nucleation of the gaseous products of motor vehicle emissions (Kittelson et al., 2004). Given the urban location of the measurement site, it is probable that local traffic emissions were responsible for maintaining concentrations in this size

range and that those emissions had been produced too recently to have been significantly affected by the surrounding dust particles.

4. Conclusions

At the peak dust time, the hourly-averaged $PM_{2.5}$ and PM_{10} values were 814 and 6460 μg m^{-3}, respectively, with the light scattering coefficient of particles, Bsp, exceeding 1000 Mm^{-1}. A linear regression analysis showed a good correlation between Bsp and both PM_{10} and $PM_{2.5}$. The PM_{10} fraction accounted for about 68% of the total mass. The particle number concentration measured by the APS exhibited a lognormal size distribution with modal and geometrical mean diameters of 1.6 and 1.9 μm, respectively. The modal mass was around 10 μm with less than 10% of the mass carried by particles smaller than 2.5 μm. The ultrafine particle number concentrations fell sharply as the dust storm passed over - from about $6x10^3$ cm^{-3} to about $3x10^3$ cm^{-3} as the dust peaked and then continued to decrease to less than $1x10^3$ cm^{-3} over the next two hours. Through our observations, we have also shown that the number concentration of ultrafine particles in the environment is significantly suppressed due to scavenging by larger particles during a dust storm. The ultrafine particle number concentration showed a power-law decrease with PM_{10} with an R^2 value of 0.73 ($p<0.01$). We believe that this is the first report of the particle size distribution in an Australian dust storm.

Acknowledgements

We would like to thank the Queensland Department of the Environment and Resource Management (DERM) for providing the hourly average PM and meteorological data for the period of the dust storm.

References

Abdulla, S.A., Al-Rizzo, H.M. and Cyril, M.M., 1988. Particle size distribution of Iraqi sand and dust storms and their influence on microwave communication systems. IEEE Trans Antennas and Propagation 36, 114-126.

Ackermann, I.J., Hass, H., Memmesheimer, M., Ebel, A., Binkowski, F.S. and Shankar, U., 1998. Modal aerosol dynamics model for Europe: Development and first applications. Atmos Environ 17, 2981-2999.

AGBM, 2010. Annual Australian Climate Statement, 2009. Australian Government Bureau of Meteorology. Issued 5 Jan 2010.

Choi, H. and Choi, D.S., 2008. Concentrations of PM_{10}, $PM_{2.5}$ and PM_1 influenced by atmospheric circulation and atmospheric boundary layer in the Korean mountainous coast during a duststorm. Atmos Res 89, 330-337.

Hefflin, B.J., Jalaludin, B., McClure, E., Cobb, N., Johnson, C.A., Jecha L. and Etzel, R.A., 1994. Surveillance for dust storms and respiratory diseases in Washington State, 1991. Arch Environ Health 49, 170-174.

Hinds, W.C., 1982. Aerosol Technology. New York, John Wiley.

Jung, C.H., Kim, Y.P. and Lee, K.W., 2002. Simulation of the influence of coarse mode particles on the properties of fine mode particles. J Aerosol Sci 33, 1201-1216.

Kittelson, D.B., Watts, W.F. and Johnson, J.P., 2004. Nanoparticle emissions on Minnesota highways. Atmos Environ 38, 9-19.

Kobayashi, H., Arao, K., Murayama, T., Iokibe, K., Koga, R. and Shiobara, M., 2007. High resolution measurement of size distributions of Asian dust using a Coulter multisizer. J Atmos Oceanic Technol 24, 194-205.

Kumar, P., Robins, A., Vardoulakis, S., Britter, R., 2010. A review of the characteristics of nanoparticles in the urban atmosphere and the prospects for developing regulatory control. Atmos Environ 44, 5035-5052.

Lei, Y.C., Chan, C.C., Wang, P.Y., Lee, C.T. and Cheng, T.J., 2004. Effects of Asian dust event particles on inflammation markers in peripheral blood and bronchoalveolar lavage in pulmonary hypertensive rats. Environ Res 95, 71-76.

Leys, J., Heidenreich, S. and Case, M., 2009. DustWatch interim report 22-23rd September. DustWatch, Department of Environment and Climate Change, NSW and Griffith University, Queensland, Australia.

Matsoukas, T. and Friedlander, S.K., 1991. Dynamics of aerosol agglomerate formation. J. Colloid Interface Sci 146, 495–506.

Mikami, M., Aoki, T., Ishizuka, M., Yabum, S., Yamada, Y., Gao, W. and Zeng, F., 2005. Observation of number concentration of desert aerosols in the South of the Taklimakan Desert, China. J Meteorol Soc Japan 83A, 31-43.

Mitchell, R.M., Campbell, S.K. and Qin, Y., 2010. Recent increase in aerosol loading over the Australian arid zone. Atmos Chem Phys 10, 1689-1699.

Morawska, L., Ristovski, Z., Jayaratne, E.R., Keogh, D.U. and Ling, X., 2008. Ambient nano and ultrafine particles from motor vehicle emissions: characteristics, ambient processing and implications on human exposure. Atmos Environ 42, 8113-8138.

Radhi, M., Box, M.A., Box, G.P., Mitchell, R.M., Cohen, D.D., Stelcer, E. and Keywood, M.D., 2010. Size-resolved mass and chemical properties of dust aerosols from Australia's Lake Eyre Basin. Atmos Environ 44, 3519-3528.

Schwartz, J., Norris, G., Larson, T., Sheppard, L., Claiborne, C. and Koenig, J., 1999. Episodes of high coarse particle concentrations are not associated with increased mortality. Environ Health Persp 107. 339-342.

Shi, J. P., Khan, A. A. and Harrison, R. M., 1999. Measurements of ultrafine particle concentrations and size distribution in the urban atmosphere. Sci Total Environ 235. 51-64.

TSI, 1997. DustTrak Aerosol Monitor, Theory of Operation. Health and Safety Application Note ITI-036. Revised 11/14/97. TSI Incorporated, St Paul MN, USA.

Wåhlin, P., Palmgren, F. and Van Dingenen, R., 2001. Experimental studies of ultrafine particles in streets and the relationship to traffic. Atmos Environ 35, S63-S69.

Wang, X., Oenema, O., Hoogmoed, W.B., Perdok, U.D. and Cai, D., 2006. Dust storm erosion and its impact on soil carbon and nitrogen losses in northern China. Catena 66, 221-227.

Wang, W., Ma, J., Hatakeyama, S., Liu, X., Chen, Y., Takami, A., Ren, L. and Geng, C., 2008. Aircraft measurements of vertical ultrafine particles over Northern China coastal areas during dust storms in 2006. Atmos Environ 42, 5715-5720.

Zhang, R., Wang, Z., Shen, Z., Yabuki, S. and Kanai, Y., 2006. Physicochemical characterization and origin of the 20 March 2002 heavy dust storm in Beijing. Aerosol and Air Quality Res 6, 268-280.

Tables

Instrument	Site	Period Operated on 23/09/2009
APS	A	16h – 24h
SMPS	A	All day
CPC	B	0h - 15h
DustTrak	B	All day
TEOM	A	All day
Nephelometer	A	All day
Met Parameters	A	All day

Table 1: The instruments, their locations and times of operation.

Figure Captions

1. Map of Australia, showing the source and dispersion of dust. All sampling was carried out in Brisbane.
2. Light scattering coefficient of particles (Bsp) as a function of time (Site A).
3. Half-hourly averaged $PM_{2.5}$ data from the DustTrak and the TEOM during the dust storm, plotted against each other.
4. Hourly average PM_{10} and $PM_{2.5}$ concentrations as a function of time (Site A).
5. Particle number (a) and volume (b) size distributions measured by the APS (Site A).
6. Ultrafine particle number concentration together with the $PM_{2.5}$ measured at Site B.
7. Hourly average ultrafine particle number concentrations as a function of the PM_{10} concentration.
8. Hourly average (a) particulate matter and (b) ultrafine particle number concentrations shown as a function of the light scattering coefficient of particles, Bsp.
9. Particle number concentration and geometrical mean diameter as measured by the APS.
10. Ultrafine particle size distributions before and during the dust storm.

Figures

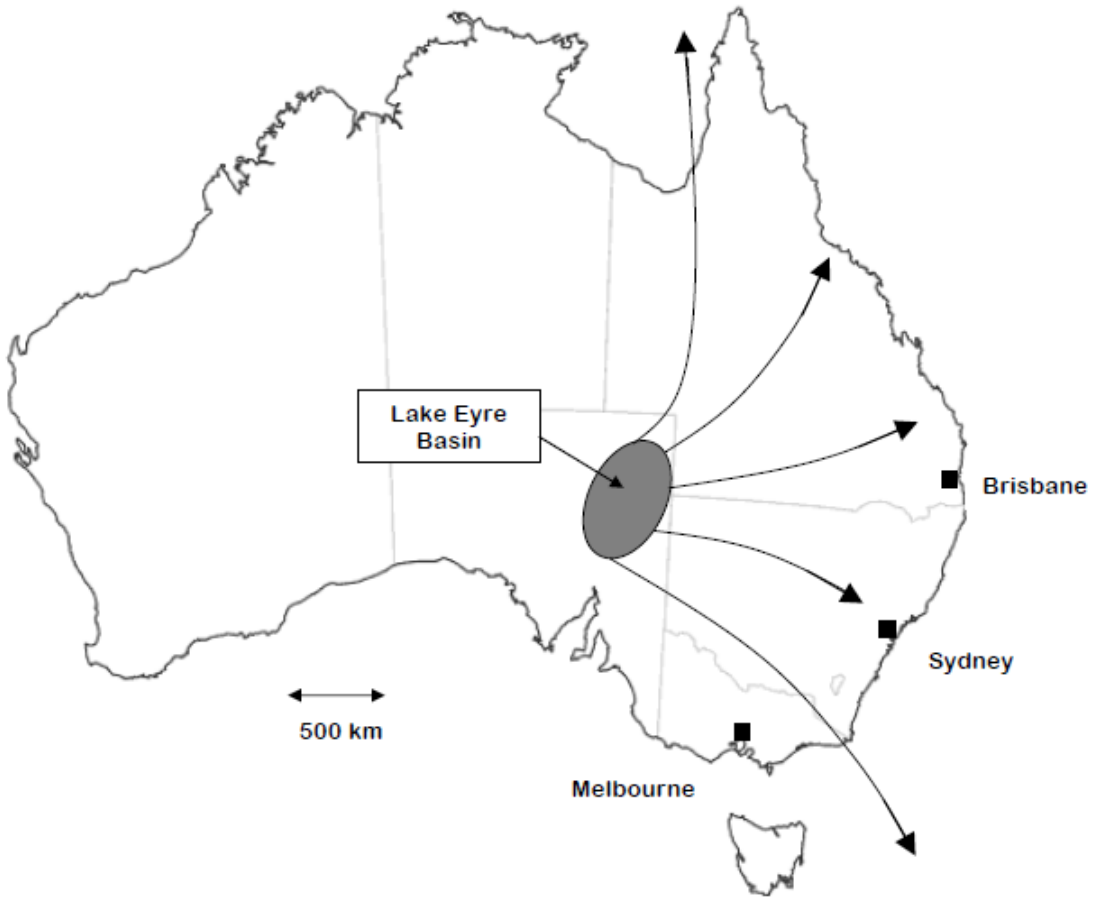

Fig 1

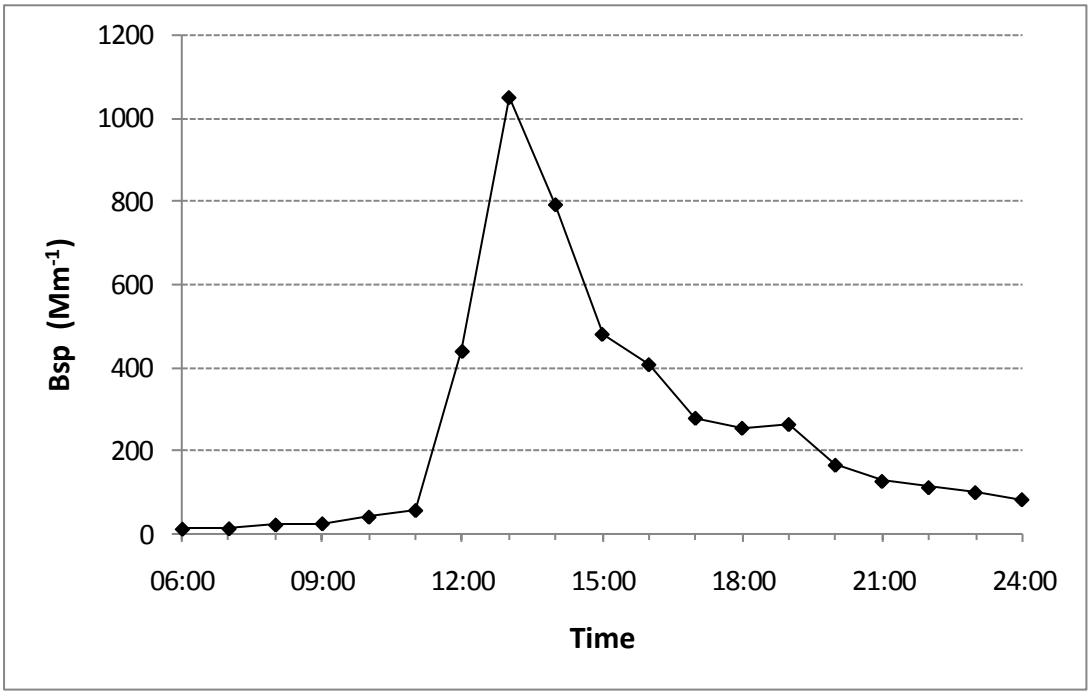
1200
1000
800
600
400
200
0
Bsp (Mm-1)
06:00
09:00
12:00
15:00
18:00
21:00
24:00
Time

Fig 2

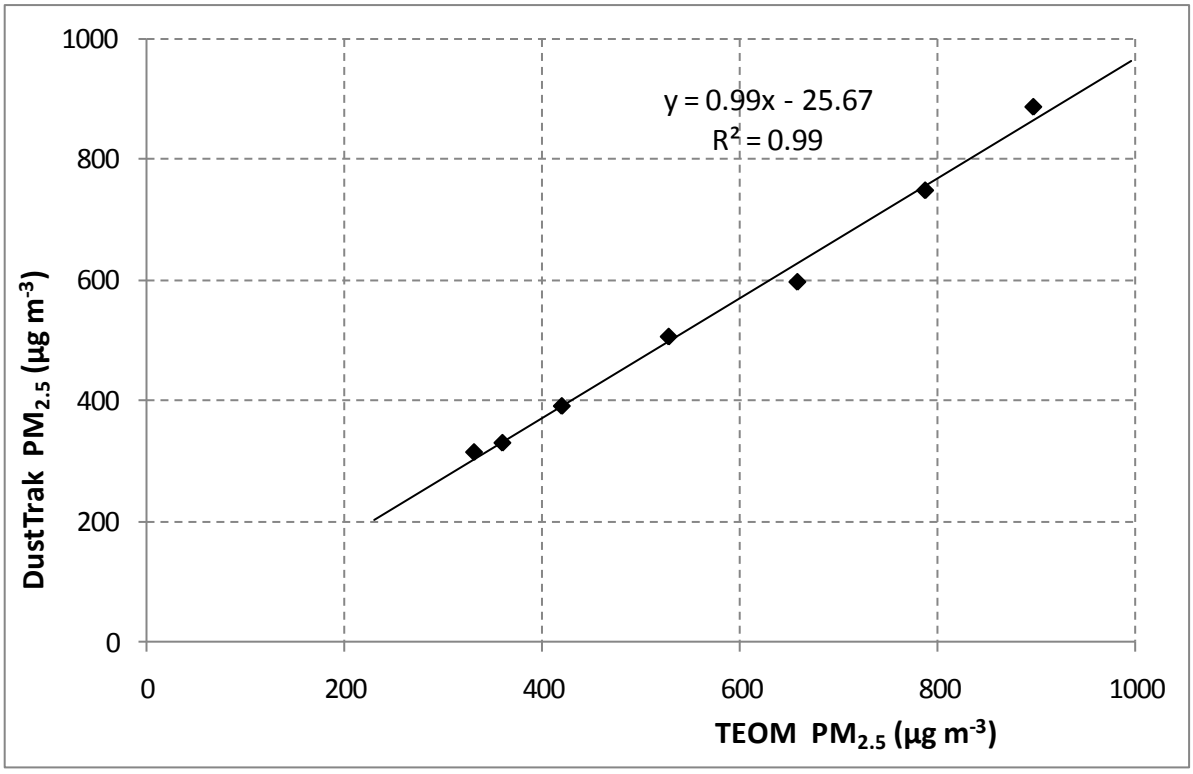
y = 0.99x - 25.67
R² = 0.99
DustTrak PM2.5 (µg m-3)
TEOM PM2.5 (µg m-3)
0
200
400
600
800
1000

Fig 3

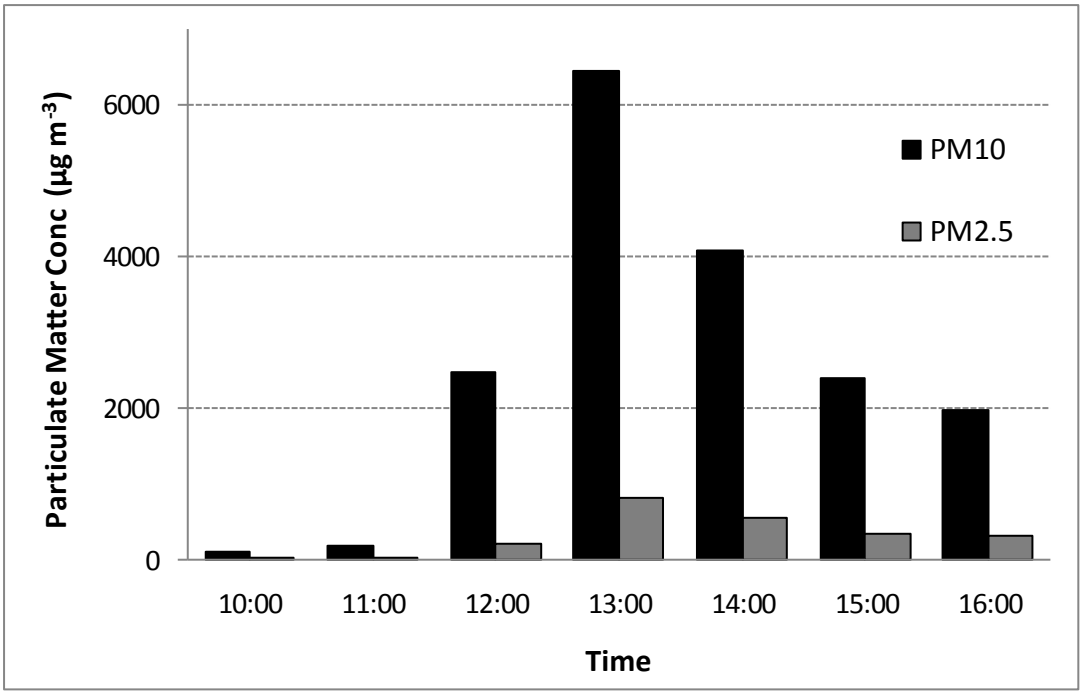
Particulate Matter Conc (µg m-3)
6000
4000
2000
0
PM10
PM2.5
10:00
11:00
12:00
13:00
14:00
15:00
16:00
Time

Fig 4

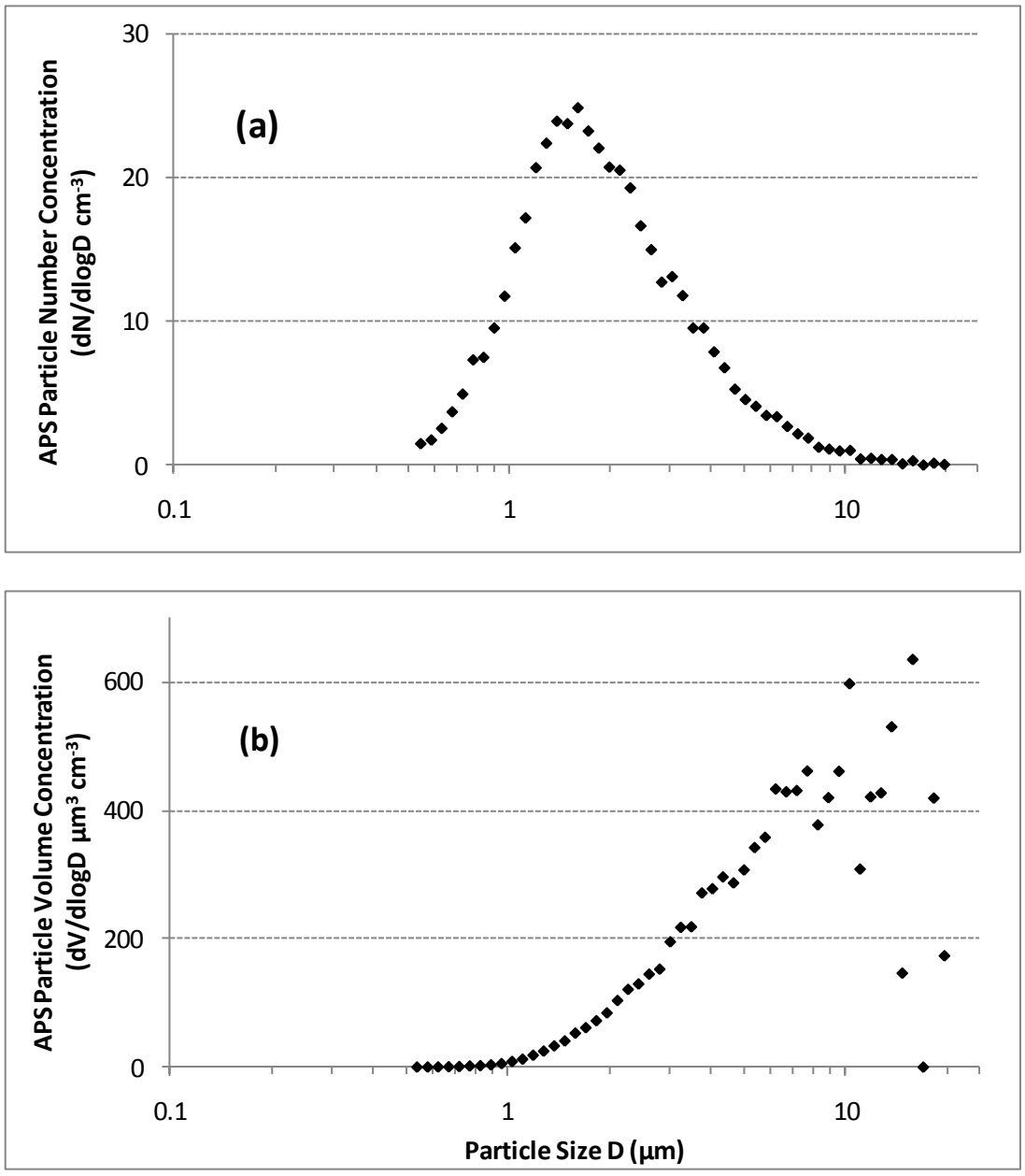
(a)
APS Particle Number Concentration (dN/dlogD cm-3)
30
20
10
0
0.1
1
10
(b)
APS Particle Volume Concentration (dV/dlogD µm3 cm-3)
600
400
200
0
0.1
1
10
Particle Size D (µm)

Fig 5

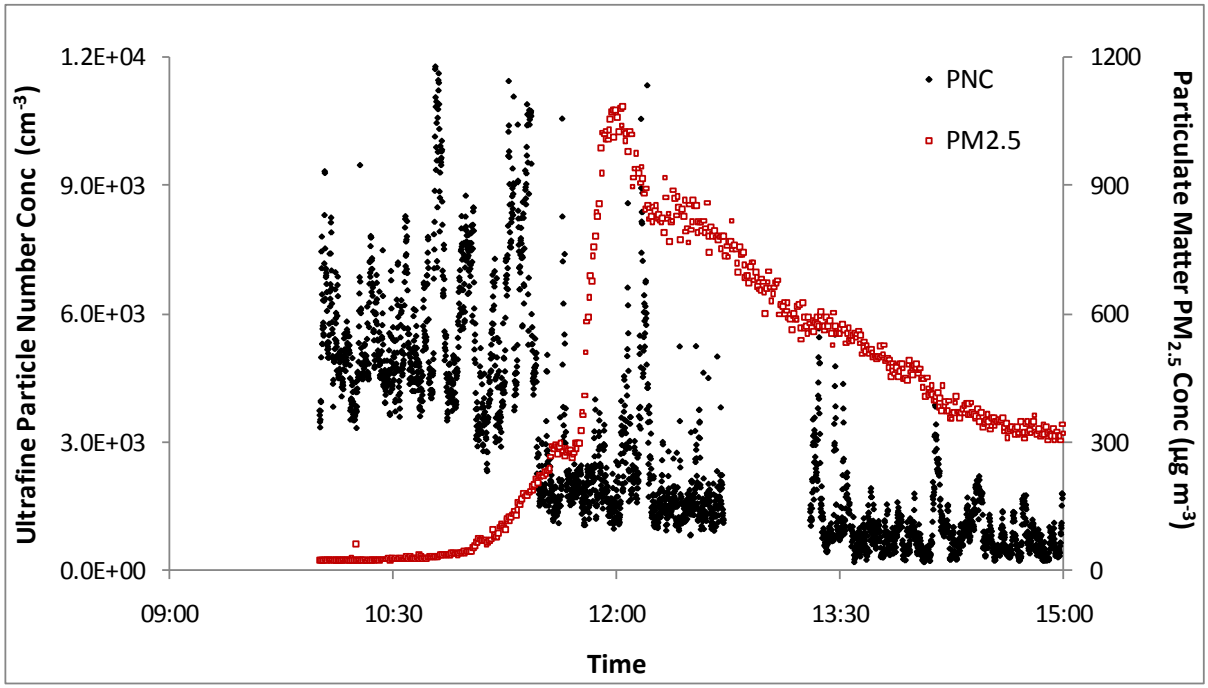
1.2E+04
9.0E+03
6.0E+03
3.0E+03
0.0E+00
Ultrafine Particle Number Conc (cm-3)
1200
900
600
300
0
Particulate Matter PM2.5 Conc (µg m-3)
PNC
PM2.5
09:00
10:30
12:00
13:30
15:00
Time

Fig 6 (Colour)

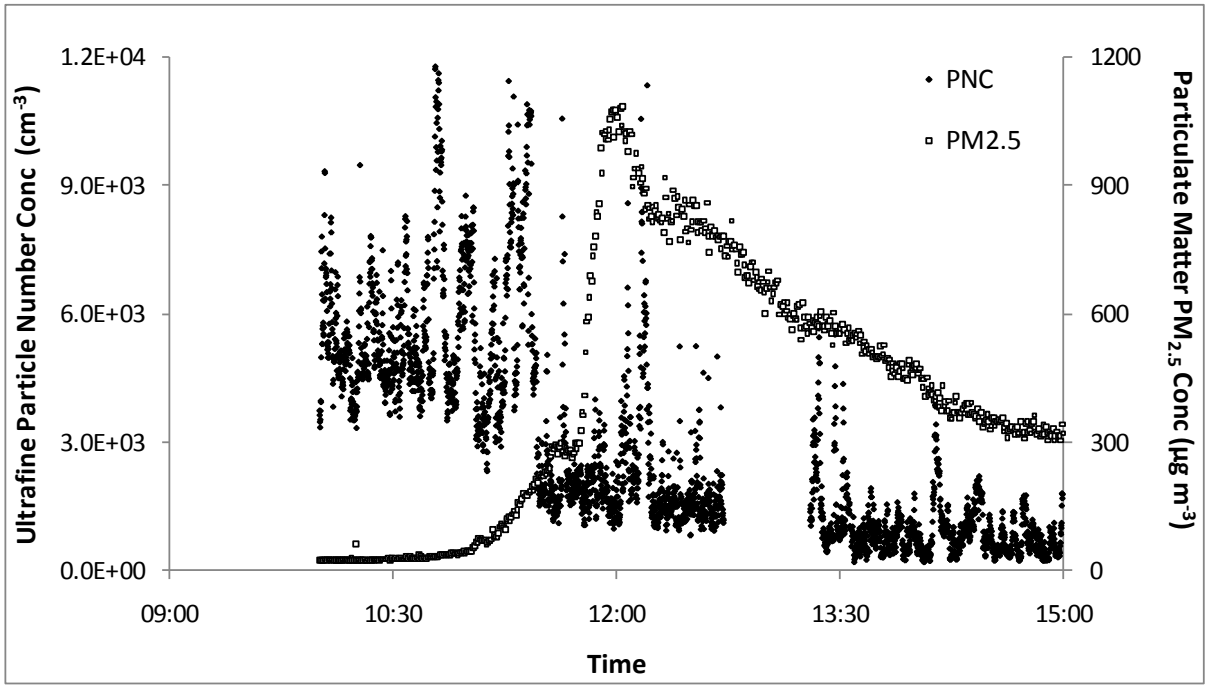
1.2E+04
9.0E+03
6.0E+03
3.0E+03
0.0E+00
Ultrafine Particle Number Conc (cm-3)
1200
900
600
300
0
Particulate Matter PM2.5 Conc (µg m-3)
PNC
PM2.5
09:00
10:30
12:00
13:30
15:00
Time

Fig 6 (B & W)

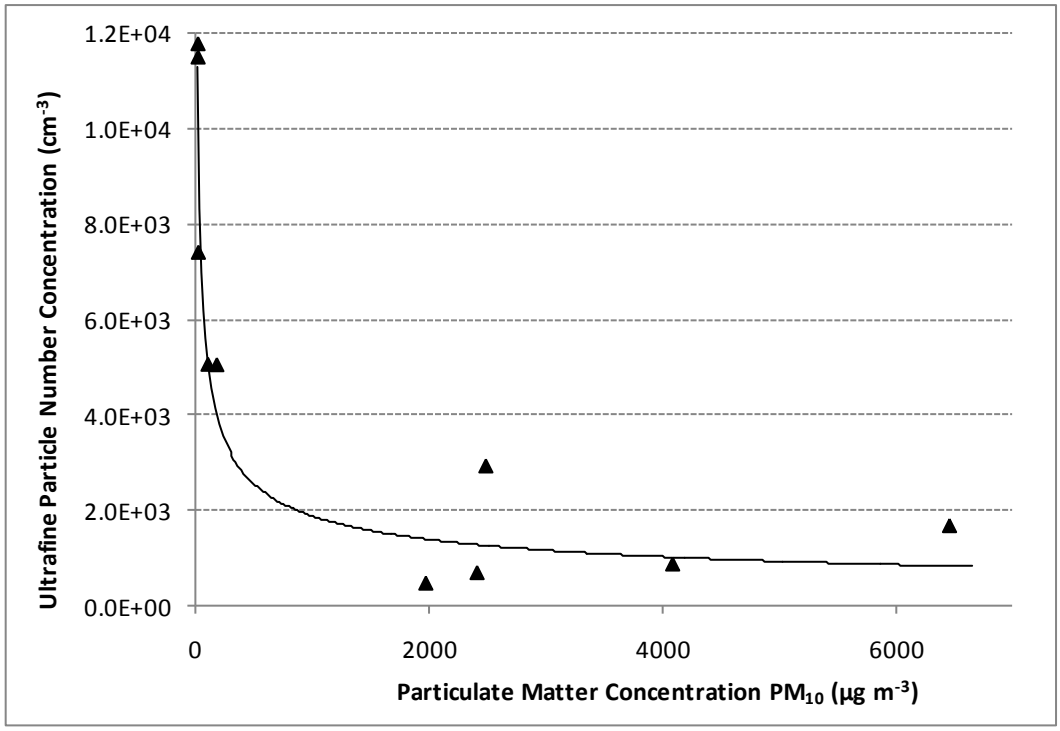
1.2E+04
1.0E+04
8.0E+03
6.0E+03
4.0E+03
2.0E+03
0.0E+00
Ultrafine Particle Number Concentration (cm-3)
0
2000
4000
6000
Particulate Matter Concentration PM10 (µg m-3)

Fig 7

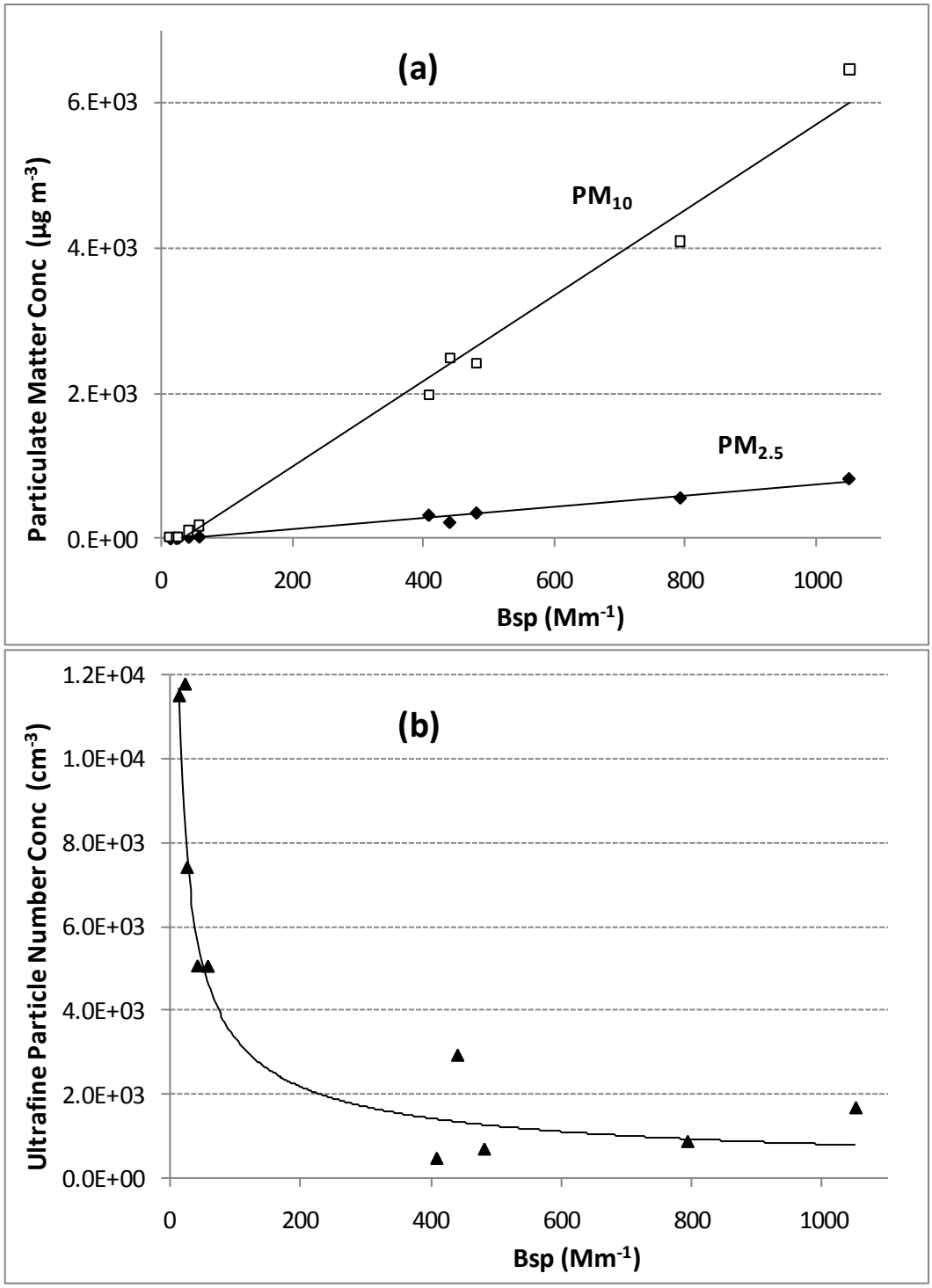
(a)
6.E+03
4.E+03
2.E+03
0.E+00
Particulate Matter Conc (µg m-3)
PM10
PM2.5
0
200
400
600
800
1000
Bsp (Mm-1)
(b)
1.2E+04
1.0E+04
8.0E+03
6.0E+03
4.0E+03
2.0E+03
0.0E+00
Ultrafine Particle Number Conc (cm-3)
0
200
400
600
800
1000
Bsp (Mm-1)

Fig 8

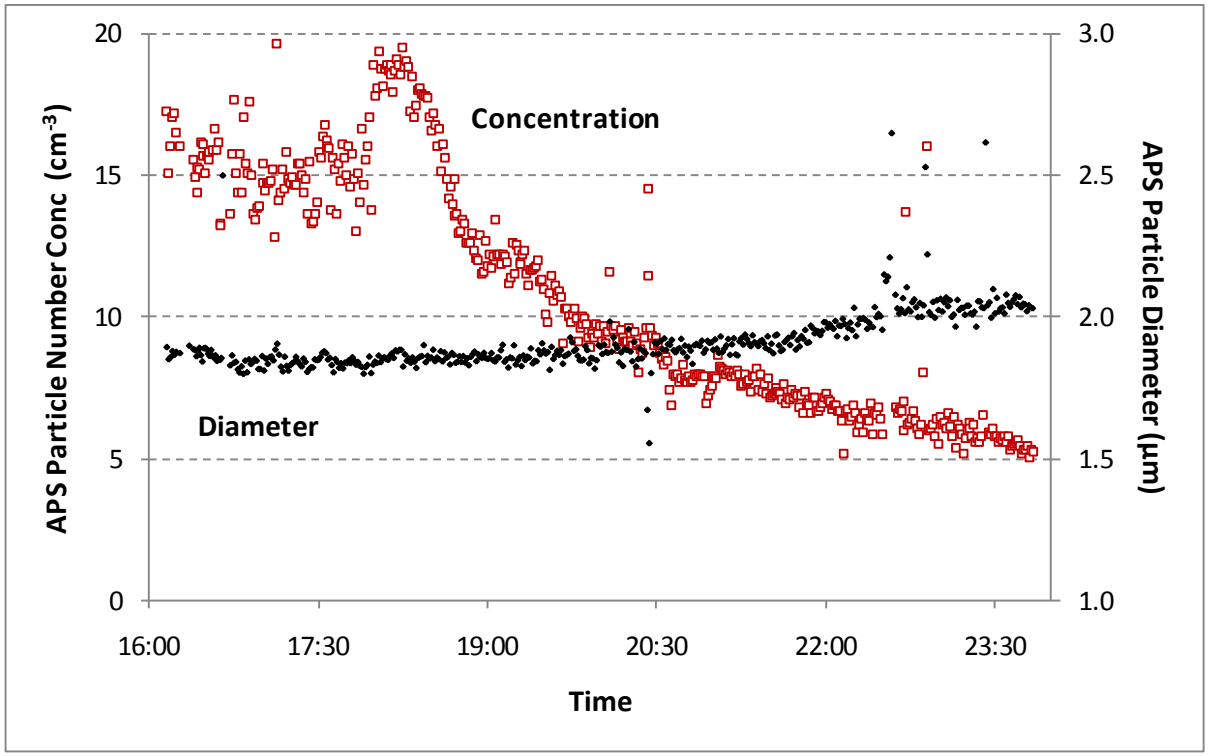
20
15
10
5
0
3.0
2.5
2.0
1.5
1.0
Concentration
Diameter
APS Particle Number Conc (cm-3)
APS Particle Diameter (µm)
16:00
17:30
19:00
20:30
22:00
23:30
Time

Fig 9 (Colour)

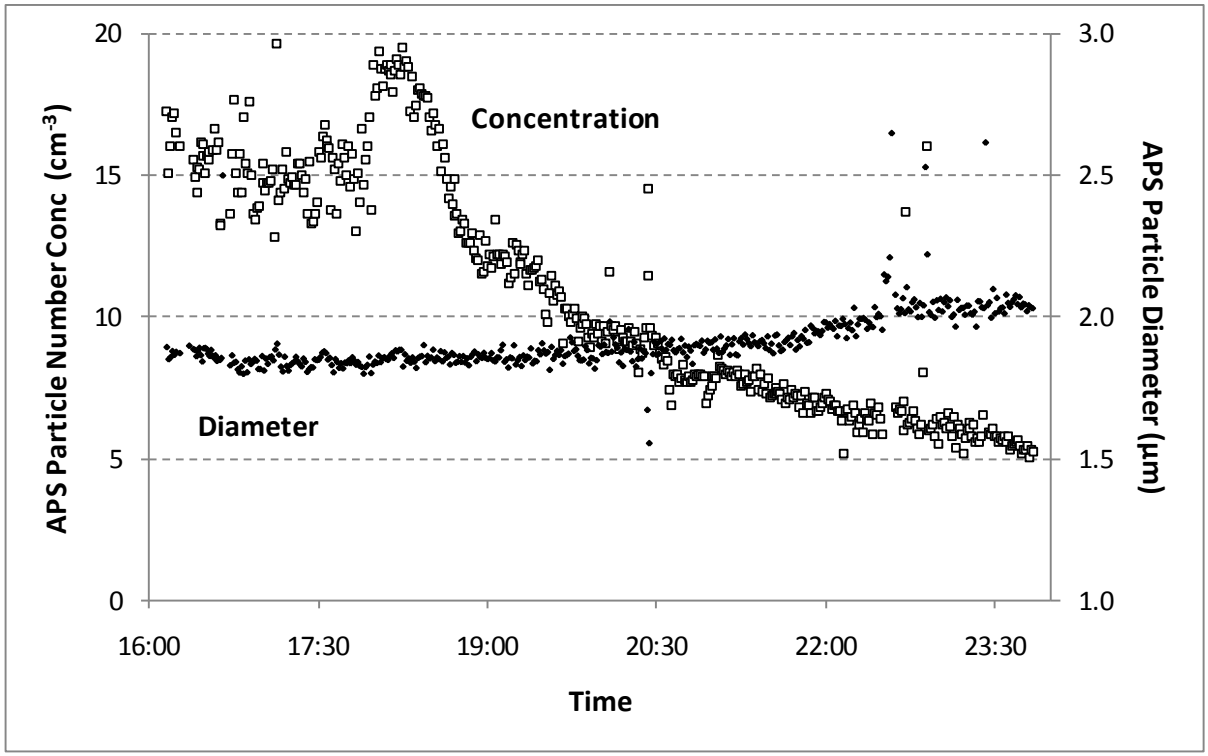
20
15
10
5
0
3.0
2.5
2.0
1.5
1.0
Concentration
Diameter
APS Particle Number Conc (cm-3)
APS Particle Diameter (µm)
16:00
17:30
19:00
20:30
22:00
23:30
Time

Fig 9 (B & W)

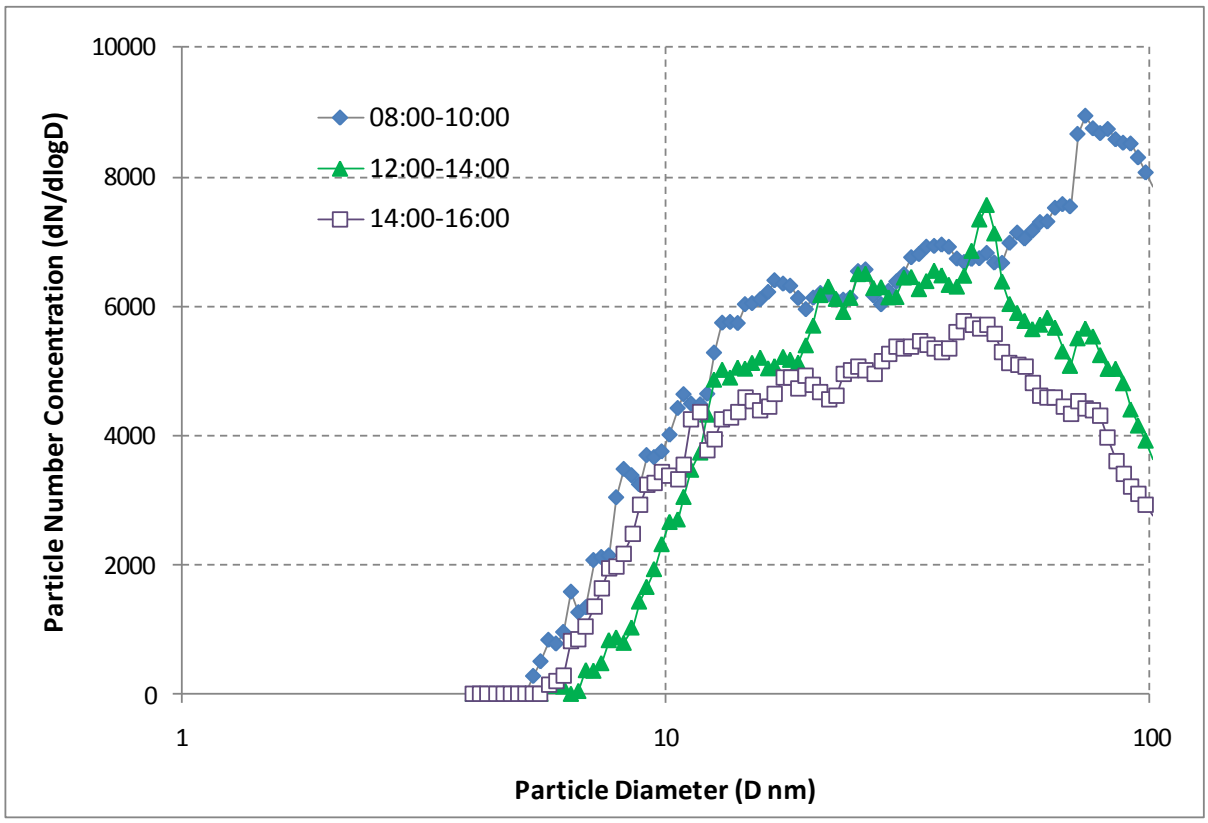

Fig 10 (Colour)

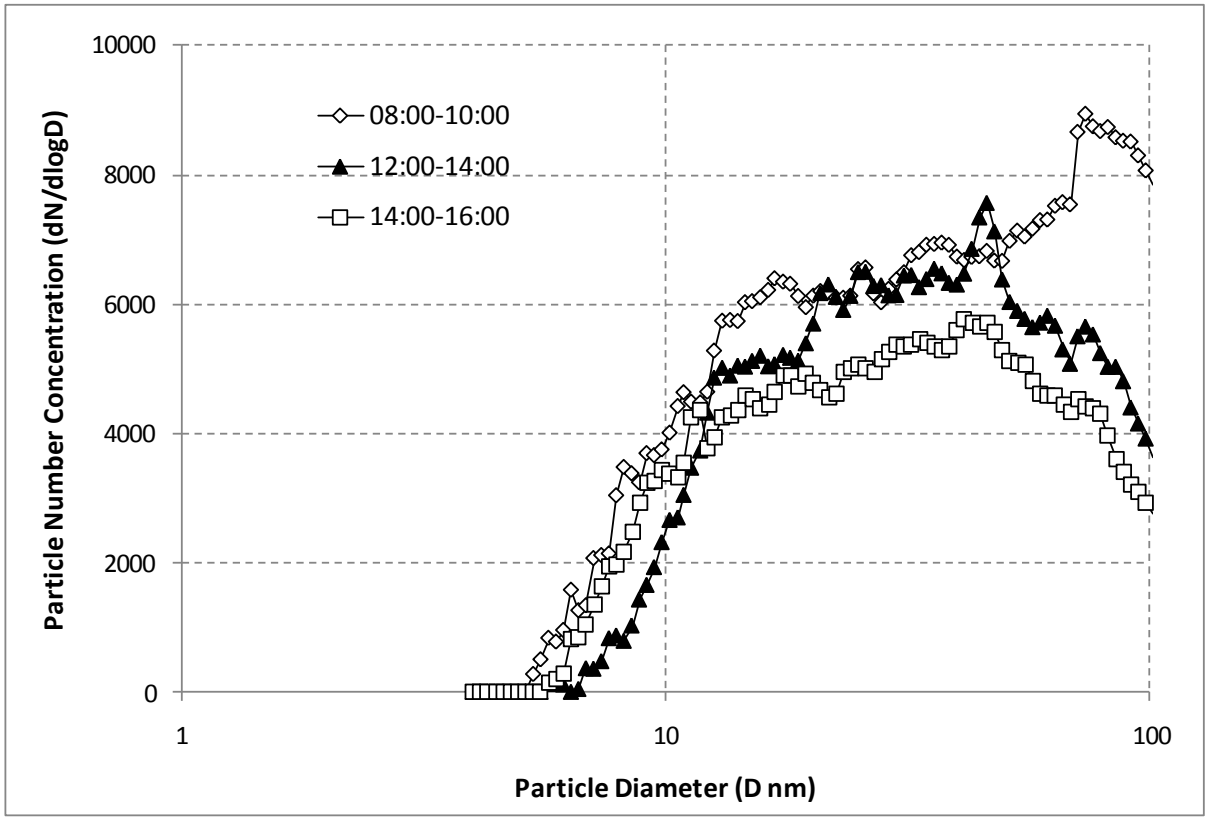
10000
8000
6000
4000
2000
0
1
10
100
Particle Number Concentration (dN/dlogD)
Particle Diameter (D nm)
08:00-10:00
12:00-14:00
14:00-16:00

Fig 10 (B & W)